JOURNAL OF AGRICULTURAL AND FOOD CHEMISTRY

Atomic Force Microscopy of Thermally Treated Myosin Filaments

TOMOHITO IWASAKI,* MASAHIRO WASHIO, AND KATSUHIRO YAMAMOTO

Department of Food Science, Rakuno Gakuen University, Ebetsu, Hokkaido 069-8501, Japan

Heat-induced morphological change in myosin filaments was observed using atomic force microscope. The thickness of fixed native myosin filament was estimated to be 95 ± 5 nm. When myosin filaments in 0.1 M NaCl at pH 6.0 were heated at 40, 55, and 70 °C for 10 min, the particulate structure appeared spirally on the surface of the filament at 40 °C, and the thickness of the filament was 75 ± 10 nm. When myosin filaments were treated at 55 °C, several filaments were formed associated with side-by-side interaction through projected myosin heads to form a strand. The surface of the strand looked knobby. The thickness of thermally denatured filaments at 55 °C was 48 ± 5 nm, and that of strands was about 80−110 nm, indicating the involvement of several filaments in a strand. The strands became to be rope-like at 70 °C, and the individual filaments in a strand were not distinguishable.

KEYWORDS: Atomic force microscope; myosin filament; thermal denaturation; gelation

INTRODUCTION

The binding property of comminuted meat products is based on heat-induced gelation of myosin. Myosin molecules are packed in the thick filaments of myofibrils under physiological condition, and the filaments dissociate into monomers with increasing ionic strength above 0.3. The transformation between filaments and monomers is reversible. Both monomeric and filamentous myosins form gels upon heating, though there is rheological difference between these two gels. The filamentous myosins form a rigid gel in comparison with monomeric myosins (*1*, *2*). In addition, the internal structures of myosin gels formed from monomers and filaments are different. Monomeric myosins form the so-called aggregated type gel and filamentous myosins form strand-type gel (*3*).

In the present study, we have focused on filamentous myosin gel that is formed at low ionic strength. Although traditional comminuted meat products usually contain over 2% salt, reducing salt concentration in meat products is expected nowadays. As describe above, salt concentration affects the state of myosins and results in a change in the type of gel. From this point of view, it is necessary to elucidate the gelation mechanism of filamentous myosins. There are some morphological studies on filamentous myosin gels so far (*1*, *4*). All of these previous studies were performed using scanning (SEM) and transmission electron microscopes (TEM).

The atomic force microscope (AFM) was developed in 1986 (*5*) and belongs to a new family of scanning probe microscopes. AFM has some advantages over SEM and TEM; namely, AFM makes possible in situ observation without metal coating, which is necessary for sample preparation of SEM, and the observation can be possible at atmospheric pressure and even in solvent. Therefore, the artifacts, including sample shrinkage, that are derived from the sample preparation for SEM and TEM or observation under vacuous condition can be avoided. Thus, AFM is recently used for the observation of various biological materials, such as polysaccharides (*6*, *7*), protein (*8*, *9*), and those associates (*10*−*13*).

In this study, we have tried to apply AFM for the morphological observation of heat-induced changes in myosin filaments. The observation was done in a solvent, so that sample shrinkage did not occur and no artifact appeared. The present results confirmed the previous reports done by TEM and SEM, and the high resolution obtained by AFM brought further information concerning heat-induced denaturation of myosin filaments.

MATERIALS AND METHODS

Chemicals. Sodium chloride and Bis-Tris were purchased from Wako Pure Chemical Industries Ltd. (Osaka, Japan) and Sigma-Aldrich Co. (St. Louis, MO), respectively. All other reagents were purchased from Nacalai Tesque INC. (Kyoto, Japan).

Protein Purification. Myosin was purified from rabbit skeletal muscle following with the method of Offer et al. (*14*). Myosin was stored as 55% ammonium sulfate precipitate at 4 °C until use. It was dialyzed against 0.5 M NaCl and clarified by centrifuge just before use. Myosin filaments were prepared by lowering the ionic strength by dialysis in 0.1 M NaCl. The final condition of the solvent was 0.1 M NaCl and 20 mM Bis-Tris (pH 6.0). Protein concentration of myosin solution was measured spectrophotometrically using an extinction coefficient at 280 nm of 0.52 (mg/mL) cm^{-1} (*15*).

Specimen Preparation. The protein concentration of myosin filament suspension was adjusted to 0.3 mg/mL. One milliliter of myosin filament suspension was incubated in a water bath at 40, 55, and 70 °C for 10 min. After incubation, each sample was immediately immersed in an ice−water bath. Thermally treated suspension at 70 °C was dispersed with pipetting. The suspensions (20 μL) were placed

* Corresponding author. Tel/Fax: +81-11-388-4834. E-mail: iwasaki@rakuno.ac.jp.

10.1021/jf0500381 CCC: $30.25
Published on Web 04/26/2005

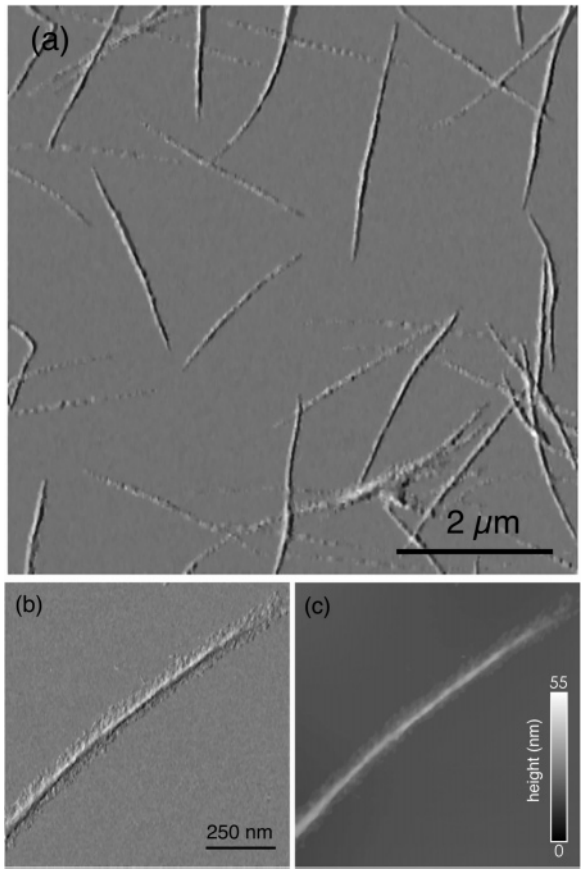

Figure 1. The AFM image of native myosin filaments. (**a**) AFM deflection image (10 × 10 μm). (**b**) Deflection image at high magnification (1 × 1 μm). (**c**) Height image corresponding to panel **b**.

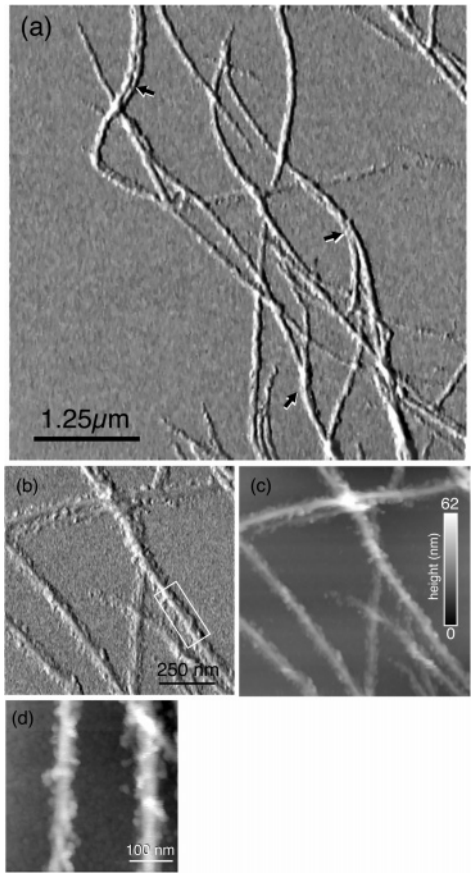

Figure 2. The AFM image of thermally treated myosin filaments at 40 °C for 10 min. (**a**) AFM deflection image (5 × 5 μm). (**b**) Deflection image (1 × 1 μm). (**c**) Height image corresponding to panel **b**. (**d**) Height image at high magnification (500 × 500 nm). The arrow indicates the portion of side-by-side interaction among filaments. The rectangular area in panel **b** shows the spiral arrangement of denatured myosin head on the surface of filament shaft.

on the surface of freshly cleaved mica and left for 5 min at room temperature. The sample was then flushed with 2 mL of 0.1 M NaCl. It was immediately immersed in a glass cell, which was filled with 0.1 M NaCl, and then imaged by AFM. Chemical fixation was done for the imaging of the native myosin filament. The sample (0.1 mg/mL) was first rinsed with 0.1 M NaCl, followed by 2.5% glutaraldehyde for 60 s. The sample was then flushed with 0.1 M NaCl before AFM imaging.

AFM Imaging. The AFM imaging was performed with a commercial instrument (SPA300HV, Seiko Instruments Inc.) in "dynamic force mode" equipped with a piezo translator with maximum $x-y$ scan range of 20 μm each and z range of 1.6 μm. A cantilevers (450 μm long; manufacturer rated spring constant, 1.6 N m^{-1}, NANOSENSER GmbH & Co. KG) with a silicon tip (radius of curvature, 15 nm) were used for imaging. "Dynamic force mode" was operated at relatively slow scan frequencies (0.2−0.5 Hz) to obtain high-quality images, and the images were captured at 512 pixels × 256 lines or 512 pixels × 128 lines.

Statistical Analysis. The data were analyzed using Kaleida Graph 3.6 software (Synergy Software, Reading, PA) for Mac OS X. Statistical analysis was performed by analysis of variance (ANOVA) and Tukey-HSD test.

RESULTS

AFM Imaging of Native Myosin Filament. AFM images of the native myosin filaments are shown in **Figure 1**. Although a satisfactory image of filaments was not obtained without chemical fixation, the native filaments were observable after fixation with 2.5% glutaraldehyde for 1 minute. The estimated length of myosin filament was 3.58 ± 0.62 μm (n = 8). This was consistent with the results obtained by transmission electron microscopy (*4*, *16*). Parts **b** and **c** of **Figure 1** show the deflection and height images of native filament, respectively. The overall thickness of filaments including crossbridge projection was 96 ± 5 nm (n = 10). The thickness of the shaft was 34 ± 9 nm (n = 13), and the expansion of cross-bridges was 30 ± 7 nm (n = 13). The filament end was flared (**Figure 1c**).

AFM Imaging of Thermally Treated Myosin Filament. Figure 2 indicates AFM images of myosin filament treated at 40 °C. The length of strands was longer than native myosin filaments, and many filaments were gathered with filament by side-by-side interaction. The arrows in **Figure 2a** indicate the region of side-by-side association. Parts **b** and **c** of **Figure 2** show the deflection and height images, respectively. Flared cross-bridge projections from the surface of myosin filaments were not observed in the thermally treated filament at 40 °C, instead the surface of filament looked particulate. The high-magnification image of the filament treated at 40 °C is shown in **Figure 2d**. As shown in **Figure 2b,d**, the particles were located spirally on the surface of filament. The thickness of filaments including projection region was 75 ± 10 nm (n = 10) and it was slightly thinner than that of native filament.

When myosin filament suspensions were heated at 55 °C, the heat-induced strands were also long as those at 40 °C (**Figure 3**a). Parts **b** and **c** of **Figure 3** show the deflection and height images of the arrowhead region in **Figure 3a**, respectively. The strands were formed by two to four filaments with side-by-side association. Two and four arrowheads in **Figure 3c** indicate the strands that consists of two and four filaments,

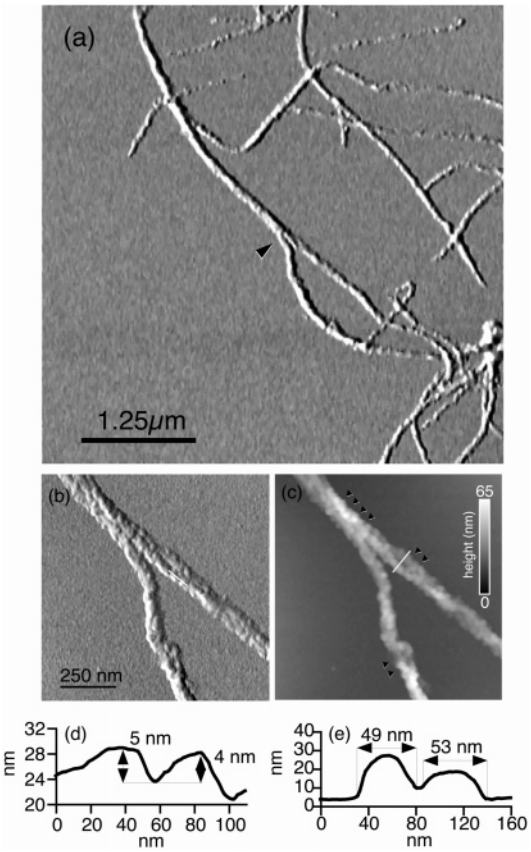

Figure 3. The AFM image of thermally treated myosin filaments at 55 °C for 10 min. (**a**) AFM deflection image (5 × 5 μm). (**b**) Deflection image (1 × 1 μm). (**c**) Height image corresponding to panel **b**. (**d**) A cross-sectional profile of panel **b**. (**e**) A cross-sectional profile of panel **c**.

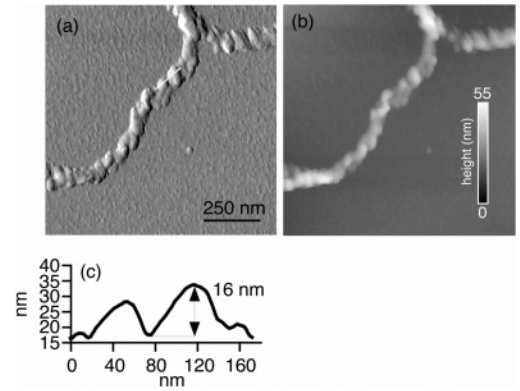

Figure 4. The AFM image of thermal treated myosin filaments at 70 °C for 10 min. (**a**) Deflection image (1 × 1 μm). (**b**) Height image corresponding to panel **a**. (**c**) A cross-sectional profile of panel **a**.

respectively. The surfaces of the strands looked knobby. **Figure 3d** shows a longitudinal profile at the position shown by a solid line in **Figure 3b**. This means the heights of the particles, and it was 4−5 nm. **Figure 3e** indicates a cross-sectional profile at a solid line in **Figure 3c**. This indicates the thicknesses of a single filament in a strand, and it was estimated to be 49−53 nm. The thickness of single filament was thinner than that of heated filament at 40 °C.

In the case of heating at 70 °C for 10 min, scanning of a wide area was difficult, because the sample was too large. Parts **a** and **b** of **Figure 4** show the deflection and height image of thermally treated filament at 70 °C. The thickness of the strand was 86 ± 9 nm (n = 10), and the strands looked rope-like.

Table 1. Filament and Strand Width (nm) at Various Temperatures[a]

	native	40 °C	55 °C	70 °C
filament	95 ± 5a	75 ± 10b	48 ± 5c	–
strand	–	–	108 ± 12a	86 ± 9ab

[a] Values not sharing a common letter differed, $p < 0.05$. Mean ± SD, n = 10.

Figure 4c shows a longitudinal profile drawn by the solid line in **Figure 4a**. The depth of the ply was 16 nm.

DISCUSSION

The ultrastructure of native and thermally treated myosin filaments has been studied by TEM and SEM so far. The new approach using AFM has the following advantages: (1) it makes possible structural analysis of protein molecules in liquid environment without dehydration and metal coating; and (2) AFM images provide quantitative information about the three-dimensional structure.

The structures of thermally denatured myosin filaments at various temperatures were different. The particles on the surface of the myosin filaments treated at 40 °C are possibly the aggregates of myosin heads, since the monomeric myosin filaments in high ionic strength were associated through their head regions and formed oligomers (*17*) and the shape of thermally treated myosin filament at 40 °C shown in **Figure 2** was similar to the image obtained by TEM (*4*). Konno et al. (*18*) reported that subfragment-2 of the myosin molecule plays an important role in the aggregation of fish myosin. The particles were spirally located on the surface of filaments, and this is derived from intrinsic arrangement of projections on the surface of native filaments (*19*, *20*). Although there is no evidence for the involvement of subfragment-2 in the heat-induced aggregation of mammalian myosins so far, it is possible that the particles on the surface of the filament involve S-2 fragments beside myosin heads, since S-2 is not fixed into the shaft of the filament. When myosin filament suspension was heated at 55 °C, the filaments were associated to form strands with side-by-side interaction among several filaments (**Figure 3**). This result is consistent with that of Yamamoto et al. (*4*). The knobby structure of the strands at 55 °C suggests the association among myosin heads on the surface of the filament shaft. The rope-like structure of the strand became remarkable at 70 °C (**Figure 4**). Each filament in a strand was no longer distinguishable (**Figure 4**).

The overall thickness of filaments and strands is summarized in **Table 1**. The thickness of a single filament became thinner with elevating temperature, and this result indicated the heat-induced association of myosin head on the shaft of the filament. The thickness of a strand also became thinner with elevating temperature. The decrease of strand thickness may be due to tight packing of myosin head clusters, which connect filaments (*17*). Tight packing of tails of myosin molecules in filament is another possible reason, since light meromyosin, which is the C terminal region of the tail, transits to random coiled structure at 55 °C (*21*). At high enough myosin concentration, such as several milligrams/milliliter, myosin filaments form a gel by heating. The resulting gel is composed with a network of strands. Rheological measurements indicate that the gel strength of filamentous myosin gel depends on heating temperature (*1*). The present study indicates structural differences in the strands with varying temperature. These structural changes in the strand probably affect the rheological property of filamentous myosin

gel. Rheological measurement of myosin strands by AFM will be reported elsewhere.

In this paper, we have demonstrated the three-dimensional morphology of native and thermally denatured myosin filaments in liquid environment by AFM. The heat-induced strands of myosin filament were formed from several filaments with side-by-side interaction of myosin heads, which were projected on the filament. The strand thickness decreased with increasing temperature. The changes in thickness of the strands are possibly due to the degree of packing of both the heads and tails of myosin filaments. The AFM is useful to analyze morphology of myosin filament and their thermally denatured strands at high-resolution with quantitative information.

ACKNOWLEDGMENT

We thank Mr. Masatsugu Shigeno (SII NanoTechnology Inc.) for his technical advice and support.

LITERATURE CITED

(1) Ishioroshi, M.; Samejima, K.; Yasui, T. Heat-induced gelation of myosin filaments at a low salt concentration. *Agric. Biol. Chem.* **1983**, *47*, 2809−2816.

(2) Hermansson, A.-M.; Langton, M. Filamentous structures of bovine myosin in diluted suspensions and gels. *J. Sci. Food Agric.* **1988**, *42*, 355−369.

(3) Hermansson, A.-M.; Harbitz, O.; Langton, M. Formation of two types of gels from bovine myosin. *J. Sci. Food Agric.* **1986**, *37*, 69−84.

(4) Yamamoto, K.; Samejima, K.; Yasui, T. Heat-induced gelation of myosin filaments. *Agric. Biol. Chem.* **1988**, *52*, 1803−1811.

(5) Binning, G.; Quate, C. F.; Gerber, C. Atomic force microscope. *Phys. Rev. Lett.* **1986**, *56*, 930−933.

(6) Morris, V. J.; Kirby, A. R.; Gunning, A. P. A fibrous model for gellan gels from atomic force microscopy studies. *Prog. Colloid Polym. Sci.* **1999**, *114*, 102−108.

(7) Ikeda, S.; Morris, V. J.; Nishinari, K. Microstructure of aggregated and nonaggregated kappa-carrageenan helices visualized by atomic force microscopy. *Biomacromolecules* **2001**, *2*, 1331−1337.

(8) Hallett, P.; Offer, G.; Miles, M. J. Atomic force microscopy of the myosin molecule. *Biophys. J.* **1995**, *68*, 1604−1606.

(9) Zhang, Y. Y.; Shao, Z. F.; Somlyo, A. P.; Somlyo, A. V. Cryo-atomic force microscopy of smooth muscle myosin. *Biophys. J.* **1997**, *72*, 1308−1318.

(10) Ikeda, S.; Morris, V. J. Fine-stranded and particulate aggregates of heat-denatured whey proteins visualized by atomic force microscopy. *Biomacromolecules* **2002**, *3*, 382−389.

(11) Yoshikawa, Y.; Yasuike, T.; Yagi, A.; Yamada, T. Transverse elasticity of myofibrils of rabbit skeletal muscle studied by atomic force microscopy. *Biochem. Biophys. Res. Commun.* **1999**, *256*, 13−19.

(12) Nyland, L. R.; Maughan, D. W. Morphology and transverse stiffness of Drosophila myofibrils measured by atomic force microscopy. *Biophys. J.* **2000**, *78*, 1490−1497.

(13) Shao, Z.; Shi, D.; Somlyo, A. V. Cryoatomic force microscopy of filamentous actin. *Biophys. J.* **2000**, *78*, 950−958.

(14) Offer, G.; Moos, C.; Starr, R. A new protein of the thick filaments of vertebrate skeletal myofibrils. *J. Mol. Biol.* **1973**, *74*, 653−676.

(15) Godfrey, J. E.; Harrington, W. F. Self-association in the myosin system at high ionic strength. II. Evidence for the presence of a monomer−dimer equilibrium. *Biochemistry* **1970**, *9*, 894−908.

(16) Yamamoto, K.; Samejima, K.; Yasui, T. The structure of myosin filaments and the properties of heat-induced gel in the presence and absence of C-protein. *Agric. Biol Chem.* **1987**, *51*, 197−203.

(17) Yamamoto, K. Electron microscopy of thermal aggregation of myosin. *J. Biochem.* **1990**, *108*, 896−898.

(18) Tazawa, T.; Kato, S.; Katoh, T.; Konno. K. Role of neck region in the thermal aggregation of myosin. *J. Agric. Food Chem.* **2002**, *50*, 196−202.

(19) Koretz, J. F. Structural studies of synthetic filaments prepared from column-purified myosin. *Biophys. J.* **1979**, *27*, 423−432.

(20) Koretz, J. F. Effects of C-protein on synthetic myosin filament structure. *Biophys. J.* **1979**, *27*, 433−446.

(21) Samejima, K.; Ishioroshi, M.; Yasui, T. Scanning Calorimetric studies on thermal denaturation of myosin and its subfragments. *Agric. Biol. Chem.* **1983**, *47*, 2373−2380.

Received for review January 7, 2005. Revised manuscript received March 24, 2005. Accepted March 31, 2005.

JF0500381